2019

Reactivity of Molybdenum and Tungsten Sulfido Complexes with First-Series Transition Metals

Khalil Mudarmah

REACTIVITY OF MOLYBDENUM AND TUNGSTEN SULFIDO COMPLEXES WITH FIRST-SERIES TRANSITION METALS

KHALIL IBRAHIM MUDARMAH

Bachelor of Science in Chemistry

Jazan University

June 2013

submitted in partial fulfillment of requirements for the degree

MASTER OF SCIENCE IN CHEMISTRY

at the

CLEVELAND STATE UNIVERSITY

AUGUST 2019

We hereby approve this thesis for

KHALIL IBRAHIM MUDARMAH

Candidate for the Master of Science in Chemistry degree for the

Department of Chemistry

and

CLEVELAND STATE UNIVERSITY'S

College of Graduate Studies by

Thesis Chairperson, Warren Christopher Boyd, Ph.D.
Chemistry Department

_____
Date

Thesis Committee Member, Aimin Zhou, Ph.D.
Chemistry Department

_____
Date

Thesis Committee Member, Xue-Long Sun, Ph.D.
Chemistry Department

_____
Date

Date of Defense: August 6, 2019

ACKNOWLEDGEMENT

First, I would like to express my worth thanks to Dr. Boyd. When I first joined Dr. Boyd's lab, I had a passion with zero expertise in Inorganic field. Dr. Boyd has helped me to enhance the skills that helped me to work with confidence in the research world. I would like to express my gratitude to my wife Wjdan for her supports, love, and patience. Also, I would thank my mother, siblings, and friends for their love and support. I am grateful to my government for granted me to complete my education overseas. Without their support, I could not even achieve my dream of studying in the USA. I also thank Dr. Wiley Youngs and his student Michael Stromyer for running many X-ray experiments for our group. I would like to thank my lab mates Ahmed, Kylin, Lakshmi, and Ashley for their help and for suggesting some ideas to solve problems. Finally, I would express my thanks to all my colleagues back home for giving advises from their expertise studying abroad that I benefited from.

REACTIVITY OF MOLYBDENUM AND TUNGSTEN SULFIDO COMPLEXES WITH FIRST-SERIES TRANSITION METALS

KHALIL IBRAHIM MUDARMAH

ABSTRACT

Ammonium tetrathiomolybdate (ATTM) is an important compound in bioinorganic chemistry, with medicinal applications. Metal complexes of sulfur-containing ligands have been widely used as building block in biology and inorganic chemistry. This project aims to increase the number of Mo-S and W-S complexes that may contribute to fields such as bioinorganic and medicinal chemistry, by the preparation of heterometallic complexes containing both Mo or S and a metal of the first transition series. The homobimetallic complex anion salts $(Et_4N)_2[Mo_2(S)_2(\mu\text{-}S)_2(edt)_2]$ (**1**) and $(Et_4N)_2[W_2(S)_2(\mu\text{-}S)_2(edt)_2]$ (**2**) have been prepared from ATTM and ammonium tetrathiotungstate (ATTW) in order to start our work. The overnight treatment of **1** and **2** with MCl_2, (M = Fe, Co, Ni, Cu) under nitrogen at elevated temperatures (84 ˚C) is hypothesized to yield trinuclear cluster anion salts. UV-visible spectra for reaction products **3**-**6** showed significantly different λ_{max} values compared with starting materials. FTIR spectra were obtained for compounds **1** and **2** for comparison with products **3**-**6**. While the spectra showed clear evidence of transformation from **1** or **2**, the structures of the products could not yet be confirmed, as attempts to obtain crystals suitable for single-crystal X-ray diffraction have so far been unsuccessful. Our future goals are to determine the structures of these reaction products, and examine their potential for medicinal and catalytic applications.

TABLE OF CONTENTS

Page

LIST OF TABLES

Table Page

LIST OF FIGURES

CHAPTER I

INTRODUCTION

Molybdenum (Mo) and tungsten (W) are transition elements of Group 6 of the Periodic Table, located in the second and third transition series, respectively. Molybdenum is known to exhibit oxidation states -2 to +6, and tungsten from +2 to +6. The 54th and 55th most abundant transition elements in the Earth's crust are molybdenum and tungsten. However, in sea water, the most abundant redox-active transition element is molybdenum. Molybdenum exists in plants, soil, water, and animals, and thus the potential bioavailability of molybdenum is greater than tungsten[1,2].

The stability of higher oxidation states generally increases down a column of the *d*-block, so Mo(VI) and W(VI) species are generally less strongly oxidizing than Cr(VI) species. Mo and W display similar chemical reactivity, though there are some notable differences. For example, $Mo(CO)_6$ reacts with a variety of reagents, such as reacting with acetic acid to yield $Mo_2(OAc)_4$, but $W(CO)_6$ does not react with acetic acid to give $W_2(OAc)_4$. Mo and W both form hexahalides such as MoF_6 and WF_6. Mo and W are nearly the same size and have similar chemical properties due to the lanthanide contraction. Mo has been found as the disulfide MoS_2 and it can be extracted from it by conversion to the oxide, followed by reduction with carbon or hydrogen. W can be

extracted *via* the fusion of its ores scheelite ($CaWO_2$) or wolframite ($FeWO_4$) with sodium hydroxide, followed by the conversion to the hydrated oxide, WO_3. Reduction of oxide with carbon or hydrogen then yields elemental W[1,3,4,5].

Molybdenum is able to form compounds with many other elements, both salts and complexes with most organic and inorganic ligands. In addition, it can form bimetallic and polymetallic compounds containing Mo–Mo bonds and/or bridging ligands. These properties make the chemistry of molybdenum both complex and fascinating, and lead to varied applications[4].

Tungsten has a very high melting point of 3420 $^{\circ}$C, and a low thermal expansion coefficient of 4.3 x 10^{-6}/°C. It is well suited for use with ceramic and glass at high temperatures because of its ability to resist thermal expansion. Tungsten's versatility makes it a very important material in applications such as light filaments, heating coils, radiation shields and plasma generators. Additionally, it is used in electrical devices like conductive coatings, circuit breakers, electronic guns, *etc*. because of its high electrical conductivity[6].

1.1. Mo and W in Living Systems

Molybdenum is not an especially abundant element in either the whole Earth or its crust. However, in the oceans, molybdenum is the most abundant of the redox-active transition metals. Living systems, from the simplest bacteria to multicellular eukaryotes like plants and animals, use molybdenum at the active centers of some enzymes that catalyze redox reactions such as in nitrogen fixation, DMSO reductase, and sulfite oxidase. Molybdenum enzymes play an important role in biogeochemistry, because of

their ability to catalyze the transformation of a variety of inorganic and organic molecules and ions[1,7,8,9].

Tungsten is known to have biological functions, and it is the only metal in the third transition series that is known to occur in enzymes, such as ferredoxin aldehyde oxidoreductase. There also exist some molybdenum-containing enzymes in which tungsten may replace molybdenum[1].

In the Earth's environments, it is well known that a high level of copper in soils leads to molybdenum deficiency, and likewise that a high level of molybdenum in soils can lead to copper deficiency, which can be medically serious. The presence of sulfate in the soil has a significant effect in ruminant animals. Molybdenum-copper antagonism is now understood to occur in the anaerobic rumen of sheep and cattle, in which sulfate is reduced to sulfide by bacterial action. Molybdenum then reacts with sulfide to form the tetrathiomolybdate ion MoS_4^{2}, which coordinates to and precipitates the copper. When high levels of molybdenum are presented, copper is precipitated and made unavailable for organisms. In a similar way, when high levels of copper are presented, molybdenum is precipitated and made unavailable for uptake.[7].

1.2. Group 6 Thiometallates Chemistry

The group 6 thiometallates consist of all anions containing a Cr, Mo, or W metal center with at least one sulfido (S^{2-}) ligand (also known as the thio ligand). The important thiometallates MoS_4^{2-} was first reported by Kruss and Corleis in late 19th century. Studies on this and similar species were begun in the late 1960s by Muller and coworkers, who examined their reactivity. The possibility using these anions in modeling biological systems has recently been expanded. The iron-molybdenum-sulfur cluster unit,

discovered by Carmer *et al.*, led to the synthesis of many polymetallic complexes, and for all of these, salts of MoS_4^{2-} were used as starting materials[10].

Group 6 sulfido complexes occur in metalloenzymes as well as in industrial processes such as hydrodesulfurization, electrocatalysis and photocatalysis. An extensive library of sulfido complexes of molybdenum and tungsten has been synthesized, providing a wide range of structural features. However, apart from tetrathiometallates MS_4^{n-} and their derivatives, complexes containing terminal sulfido ligands with M–S multiple bonding are less common than complexes containing the terminal oxido (also known as oxo) ligand O^{2-}. The metal-sulfur bond can react in either a nucleophilic or electrophilic fashion. Especially in the case of complexes with molybdenum-sulfur bonds, these species can have biological applications. Also, thiometallates can themselves act as ligands to other metals, in reactions such as the formation of polymetallic complexes [1,5].

Mononuclear sulfido complexes having two or three M–S bonds are rare. There are few effective synthetic pathways to such complexes, and the difficulty is due to the following reasons: First, sulfur containing ligands have a tendency to bridge multiple metal atoms, which leads to polymetallic complexes. Second, metal sulfido complexes can undergo redox reactions in solution by intermolecular electron transfer processes, leading to S–S bond formation and concomitant reduction of metal centers. For example, MS_4^{n-} (M= Mo, W) anions are readily transformed to different polythiomolybdate and polythiotungstate anions. The reason is that the formation of sulfido complexes is predominantly carried out under reducing conditions, which favors metal-metal bond formation due to the fact that sulfurization reagents, such as alkali metal sulfides and

alkaline earth metal sulfides, act as strong bases. However, metals in high oxidation state do not have enough *d* electrons to form strong metal-metal bonds. Thus, it remains challenging to synthesize mononuclear sulfido complexes of molybdenum and tungsten. However, Enemark and Young have isolated mononuclear sulfido complexes of molybdenum and tungsten using a bulky (pyrazolyl) borate auxiliary ligand[11].

1.3. Importance of ATTM in Biological Systems

Wilson's disease is a rare, autosomal, recessive genetic disorder of copper metabolism leading to copper accumulation in both the liver and extrahepatic organs such as the brain and cornea. It was first described as a syndrome by Kinnier Wilson in 1912. This disease affects between 1 in 30,000 and 1 in 100,000 individuals. It has been found that ammonium tetrathiomolybdate (ATTM), $(NH_4)_2MoS_4$, is an effective initial treatment for Wilson's disease[12].

Ceruloplasmin is a copper protein which was found to be a molecular link between copper and iron metabolism[13,14]. In Wilson's disease, copper toxicity is caused by free copper, which is not bound to ceruloplasmin in the blood. Researchers at the University of Michigan found that ATTM could strongly control free copper levels over 8 weeks of treatment in 55 patients in an open-label trial, and was a good control of free copper levels over 8 weeks treatment in a 44-patient double-blind trial[15].

ATTM is a superior and unique anti-copper drug for the treatment of the neurologic presentation of Wilson's disease. In one study, ATTM was tested on mouse cancer models to see if tumor growth would be inhibited based on an antiangiogenic effect, and it was found that ATTM was very effective in these models. Also, ATTM can inhibit copper-dependent cytokines involved in inflammation, leading to its displaying

anti-inflammatory properties. These properties may be involved in ATTM's anticancer effect, since cancers attract inflammatory cells that release a plethora of additional proangiogenic agents[16]. In another study, it was shown that tetrathiomolybdate can rapidly remove copper from metallothioneins, a family of small, cysteine-rich metal-binding proteins which are significant for zinc and copper homeostasis and protection against oxidative stress and toxic heavy metals. Tetrathiomolybdate treatment led to an increase in bile and blood copper levels in Long-Evans Cinnamon rats[17].

Although copper is an essential metal for many biological functions, excessive amounts can stimulate inflammation and oxidative stress. As ATTM is a copper chelator for the treatment of Wilson's disease, and lowers the severity of autoimmune arthritis in mice, a study on the effect of ATTM on a mouse model for psoriasis was reported. It was found that ATTM significantly decreased epidermis thickness and the expression of ki-67, an antigen that is expressed in all vertebrates and is used as a marker of proliferation used for grading tumors, in inflamed skin. Moreover, ATTM reduced the skin cytokine levels and systemic inflammation, and inhibited activation in keratinocytes and splenocytes with a reduction in phosphorylation in Erk1/2 and STAT 3. These results were evidence that ATTM can inhibit psoriasis in a mouse model[18,19].

1.4. Reactivity of $(NH_4)_2 MS_4$

ATTM has been shown to be an effective antidote for poisoning by certain metal ions. Also, replacement of the ammonium cation by sodium, resulting in the salt Na_2MoS_4, reduced the acute toxicity (LD_{50} value) which is significant for clinical trials of these salts[20].

Molybdenum-sulfur (Mo-S) species are significant in both metalloenzymatic and industrial catalytic systems. Due to this importance, a various studies of the chemistry of molybdenum in sulfur coordination environments have been conducted. The binary Mo-S anions, such as MoS_4^{2-}, $Mo_2S_8^{2-}$, $Mo_2S_{10}^{2-}$, $Mo_2S_{12}^{2-}$, $Mo_3S_9^{2-}$, and $Mo_3S_{13}^{2-}$ constitute an interesting class of Mo-S complexes, comprising a remarkable range of stoichiometries, coordination geometries, oxidation states, and bonding modes. Moreover, these anions have been significant in the investigation of the chemical reactivity and redox properties of molybdenum-sulfur complexes and have proved to be convenient precursors for synthesizing other Mo-S species, particularly those containing the *syn*-$Mo_2S_4^{2+}$ core structure[21].

Compared to Mo-S species, the chemistry of sulfur-coordinated tungsten complexes has encountered less attention, despite the activity of tungsten sulfide hydrotreating catalysts. Such catalysts are used in hydrogenation processes that saturate unsaturated hydrocarbons and remove contaminants such as sulfur- and nitrogen-containing organic compounds in fossil fuels[22]. Biological roles for tungsten have recently been uncovered[21]. Thus far, only a few binary W-S anions have been described and of these, only the tetrathiotungstate dianion, WS_4^{2-} has been shown general synthetic interest. Similarly, complexes consisting the $W_2S_4^{2+}$ subunit remain unusual [21].

The salts $(NH_4)_2MS_4$ (M = Mo, W) have been found to decompose first to MS3 and then to MS2 upon heating to 220-240 °C. These decompositions result from a complex series of reactions. Muller and coworkers found that the final product of tetrathiomolybdate decomposition was MoS2. On the other hand, the final product for

tetrathiotungstate decomposition was a mixture of WS2 and WO2, formed in the presence of O_2, with the average stoichiometry $WO_{0.5}S_{1.75}$[23].

Cohen and Stiefel have reported rational syntheses of dimetallic tungsten(V) and molybdenum(V) sulfide complexes having high sulfur-to-metal ratios. The $M_2S_{12}^{2-}$ anions (M = W or Mo) have been prepared in high yields as their tetraethylammonium (NEt_4^+) salts from the reactions of elemental sulfur with $(NH_4)_2 MS_4$ in hot N,N-dimethylformamide (DMF). By single-crystal X-ray diffraction methods, $(NEt_4)_2W_2S_{12}$ was characterized. The structure of the $W2S12^{2-}$ anion contains of a syn-$W_2(S)_2(\mu\text{-}S)_2^{2+}$ core coordinated by two bidentate tetrasulfido (S_4^{2-}) ligands. An analogous structure such as $Mo_2(S)_4(S_4)_2^{2-}$ was observed for $(NEt_4)2Mo_2S_{12}$. Both $(NEt_4)_2W_2S_{12}$ and $(NEt_4)_2Mo_2S_{12}$ have been found to be convenient precursors for the synthesis of other dimetallic complexes[21].

1.5. Reactivity of Dimetallic Molybdenum(V) Sulfide Complexes

Wei and coworkers found that the reaction of $(Et_4N)_2[(edt)_2Mo_2(S)_2(\mu\text{-}S)_2]$ (edt^{2-} = ethane-1,2-dithiolate) with equimolar amounts of CuBr gave rise to the hexanuclear cluster anion salt $(Et_4N)_2[(edt)_2Mo_2(\mu\text{-}S_3)(\mu_3\text{-}S)Cu]_2 \cdot 2CH_2Cl_2$ (Figure 1). Also, the treatment of $(Et_4N)_2[(edt)_2Mo_2(S)_2(\mu\text{-}S)_2]$ with two equivalents of CuBr in the presence of 1,2-bis(diphenylphosphino)methane (dppm) and pyridine (py) ligands afforded two neutral clusters $[(edt)_2Mo_2O_2(\mu\text{-}S)_2Cu_2(dppm)_2]$ and $[(edt)_2Mo_2O_2(\mu\text{-}S_3)(\mu_3\text{-}S)Cu_2\ (py)_4]$, respectively (Figure 1). The oxygen in these two species probably came from either O_2 in air or small amount of water in the solvents used as Wei and coworkers reported. Finally, the reaction of $(Et_4N)_2[(edt)_2Mo_2S_2(\mu\text{-}S)_2]$ with 2 equivalents of CuBr followed by the

addition of a 2:1 mixture of py and dppm formed another neutral tetranuclear cluster, $[(edt)_2Mo_2(\mu\text{-}S)_2\ (\mu_3\text{-}S)\ Cu_2(dppm)(Py)]\cdot 6Py$[24] (Figure 1).

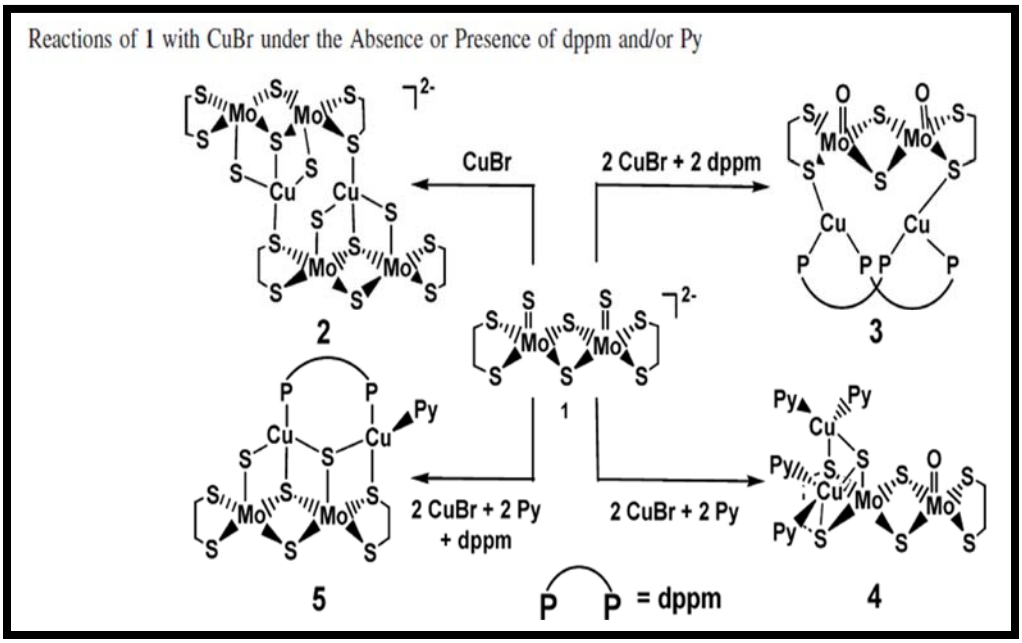

Figure1: Products from the reaction of $(Et_4N)_2[(edt)_2Mo_2S_2(\mu\text{-}S)_2]$ with CuBr in the presence or absence of dppm and/or py[24]

Another tetranuclear cluster was prepared by Wang and You in 2009 (figure 2). The reaction of $(Et_4N)_2[(edt)_2Mo_2(S)_2(\mu\text{-}S)_2]$with two equivalents of $Ag(CH_3CN)_4ClO_4$ in the presence of (dppm) afforded $[Ag_2Mo_2(edt)_2(S)_2(\mu\text{-}S)_2(dppm)_2]\cdot 3DMF$ [25].

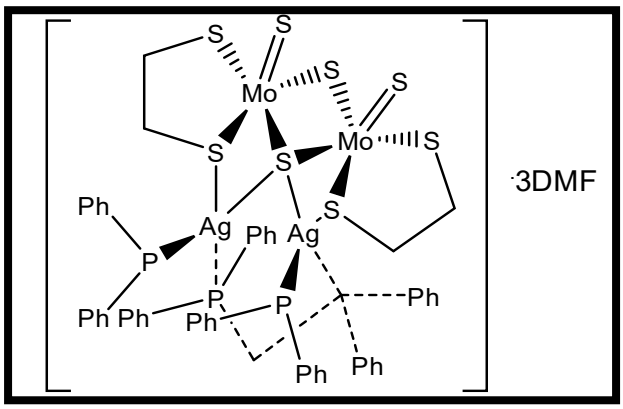

Figure 2: Structure of $[Ag_2Mo_2(edt)_2(S)_2(\mu\text{-}S)_2(dppm)_2]\cdot 3DMF$ [25]

In 2009, You and Liu investigated the treatment of $(Et_4N)_2[(edt)_2Mo_2(S)_2(\mu\text{-}S)_2]$ with two equivalents of CuCN, and found that this gives rise to the anionic tetranuclear cluster salt $(Et_4N)_2[Cu_2Mo_2(edt)_2(S)_2(\mu\text{-}S)_2(CN)_2]$. Figure (3)[26].

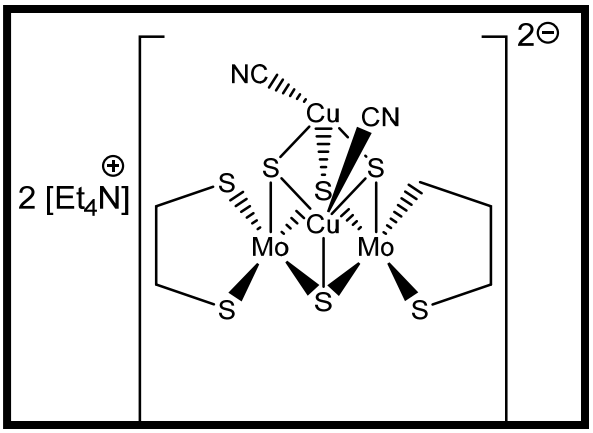

Figure 3: structure of $(Et_4N)_2[Cu_2Mo_2(edt)_2(S)_2(\mu\text{-}S)_2(CN)_2]$[26]

The chemistry of sulfido-bridged dimetallates $[(edt)_2M_2(S)_2(\mu\text{-}S)_2]^{2-}$ (M = Mo, W) with different transition metals has been widely investigated. However, the reaction of $(Et_4N)_2[(edt)_2M_2(S)_2(\mu\text{-}S)_2]$ (M = Mo, W) with first-row late transition elements in their +2 oxidation states, such as Fe(II), Co(II), Ni(II), or Cu(II) salts, is not well known. We wished to examine the reactivity of $(Et_4N)_2[(edt)_2M_2S_2(\mu\text{-}S)_2]$ with these first-row transition elements, with the possible eventual use of new species formed in catalysis or medicine. Our goal is to increase the number of Mo-S and W-S complexes that may contribute to fields such as bioinorganic and medicinal chemistry.

CHAPTER II

MATERIALS AND EXPERIMENTAL METHODS

Air- and moisture-sensitive reagents and products were manipulated under dry nitrogen in an MBraun Labstar Pro glovebox. Reactions performed in the glovebox used glassware that was oven-dried at 160˚C. Hexane, acetonitrile (CH_3CN), diethyl ether (Et_2O), and dichloromethane (DCM) were deoxygenated by sparging with dry nitrogen and then dried by passage through activated alumina in an MBraun MB-SPS solvent purification system. Dry, oxygen-free *N*,*N*-dimethylformamide (DMF) was purchased and used in the glove box without further purification. Ammonium tetrathiomolybdate $(NH_4)_2MoS_4$ (ATTM), ammonium tetrathiotungstate $(NH_4)_2WS_4$ (ATTW), tetraethylammonium bromide Et_4NBr, ethane-1,2-dithiol, and anhydrous $FeCl_2$ $CoCl_2$, $NiCl_2$, and $CuCl_2$ were commercially obtained and used without further purification. All other solvents were used in air outside of the glovebox.

Reaction mixtures were stirred using a Teflon-coated magnetic stir bar. When heat was required, reaction mixtures were set up in the glovebox in a Schlenk tube with a Teflon stopcock, tightly sealed, and heated in a silicone oil bath in the fume hood, before being cooled, returned to the glovebox, and worked up. All UV-visible spectra were

obtained on a Shimadzu UV-2600 spectrometer. UV-visible spectra were performed on samples in quartz cuvettes (path length 1.2 cm), and all solutions for UV-visible spectroscopy were prepared open to air.

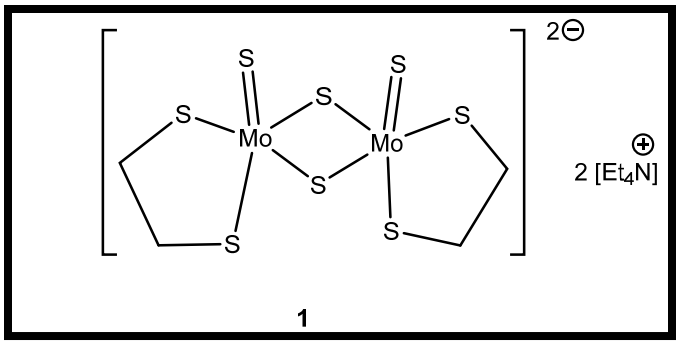

Figure 4: Structure $(Et_4N)_2[Mo_2(S)_2(\mu\text{-}S)_2(edt)_2]$, edt = ethane-1,2-dithiolato

2.1. Preparation of Compound 1: $(Et_4N)_2[Mo_2(S)_2(\mu\text{-}S)_2(edt)_2]$

The procedure reported by Pan and coworkers[27] was followed, with minor modification. In the glovebox, 1.29 g (4.9 mmol) of ATTM was added to a 100-mL Schlenk tube containing a stir bar. Next, 0.63 ml (7.5 mmol) of ethane-1,2-dithiol was dissolved in 32 ml of degassed DMF, and then added to the Schlenk tube to dissolve ATTM, yielding a red solution. The Schlenk tube was sealed tightly, removed from the glovebox, and heated in a silicone oil bath with stirring for 90 minutes at 90 ˚C, after which the red reaction mixture was cooled and returned to the glovebox without being opened. In the glovebox, 1.5 g (7.2mmol) of Et_4NBr was added. After all the Et_4NBr dissolved, the reaction was filtered. Diethyl ether was added to the filtrate to the point of incipient precipitation, and the filtrate was allowed to cool at -30 ˚C overnight. The next day, red-orange crystals formed, which were filtered, washed by diethyl ether, and dried under vacuum, yielding 1.4 g product (73% 1.83 mmol).

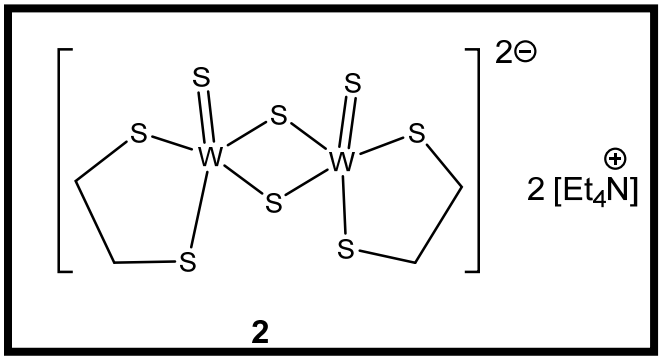

Figure 5: Structure of $(Et_4N)_2[W_2(S)_2(\mu\text{-}S)_2(edt)_2]$

2.2. Preparation of Compound 2: $(Et_4N)_2[W_2(S)_2(\mu\text{-}S)_2(edt)_2]$

The procedure reported by Pan and coworkers[27] was followed, with minor modification. In the glovebox, a solution of 0.8 g (2.3 mmol) ATTW in 15 mL DMF was added to a solution of 0.3 mL ethane-1,2-dithiol (3.6 mmol) in 10 mL DMF in a Schlenk tube with magnetic stir bar, yielding a yellow solution. The reaction mixture was tightly sealed, removed from the glovebox, and heated in a silicone oil bath with stirring for 120 min at 120 ˚C. The color changed gradually from yellow, to orange, to red. After this time, the reaction mixture was cooled to room temperature and returned to the glovebox without being opened. In the glovebox , 0.8 g (3.8mmol) Et_4NBr, was added to the reaction mixture. After all the Et_4NBr dissolved, diethyl ether was added to the reaction mixture to precipitate an orange-red powder. This powder was filtered and washed with methanol to remove a white solid impurity, and dried under vacuum to yield 0.56 g product (50% 0.59 mmol).

In an effort to prepare heterotrimetallic complexes, **1** or **2** was treated with a metal(II) chloride from the first transition series $M'Cl_2$, where M′ = Fe, Co, Ni, or Cu, with the proposed reaction shown below.

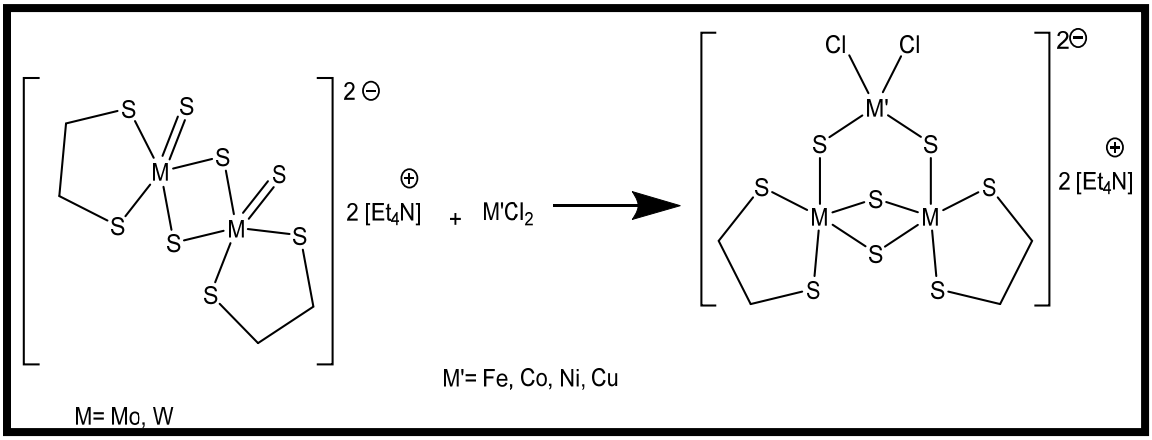

Figure 6: Synthesis of heterometallic complexes

2.3. Treatment of Compound 1 with $FeCl_2$

To a 100-mL Schlenk tube with stir bar was added a solution of 98 mg (0.1 mmol) **1** in 10 ml of CH_3CN. To this solution was slowly added a solution of 19 mg (0.1 mmol) $FeCl_2$ in 5 mL CH_3CN. The color changed gradually from orange-red color to a darker color. The reaction mixture was removed from the glovebox and heated overnight (20-24 h) at about 84˚C in a silicone oil bath. After the reaction mixture was cooled to room temperature the following day, the solvent of the mixture was removed on the Schlenk line system without exposing the mixture to air, and the solid crude product was returned to the glovebox. To the crude product was added 10 mL CH_2Cl_2, and the mixture was filtered, giving a red-brown filtrate. The filtrate was collected, 10 mL hexane was gently layered on top, and the mixture was placed in the glovebox freezer at -30 ºC . Crystals were formed within 2 to 4 days in the freezer. The supernatant was removed, and the crystals were washed by hexane and dried under vacuum yielding 0.019 g product, the structure of which is proposed to be compound **3** below.

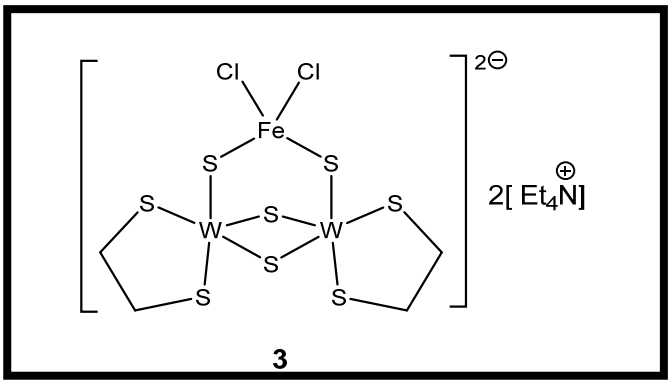

Figure 7: Structure of compound 3

2.4.Treatment of Compound 2 with $CoCl_2$

In the glovebox, to a 100-mL Schlenk tube with stir bar was added a solution of 95 mg (0.1 mmol) **2** in 10 mL of CH_3CN. To this solution was slowly added a solution of 21 mg (0.1 mmol) $CoCl_2$ in 5 ml CH_3CN. The color changed gradually during the addition from orange-red to a darker color; the exact color of the darker solution was difficult to determine. The Schlenk tube was tightly sealed, and the reaction mixture was removed from the glovebox was heated overnight (20-24 h) at about 84 ˚C in a silicone oil bath. The following day, the reaction mixture was cooled to room temperature, the solvent was removed on the Schlenk line without exposing the mixture to air, and the crude solid product was returned to the glovebox. To the crude product was added 10 mL CH_2Cl_2, and the mixture was filtered, giving a red filtrate. To the filtrate was then added 10 mL hexane, gently layered, and the mixture was put in the glovebox freezer at -30 ˚C, giving green crystals in several days. The supernatant was removed, and the crystals were washed by hexane and dried under vacuum, yielding 0.027 g product, with **4** as the proposed structure.

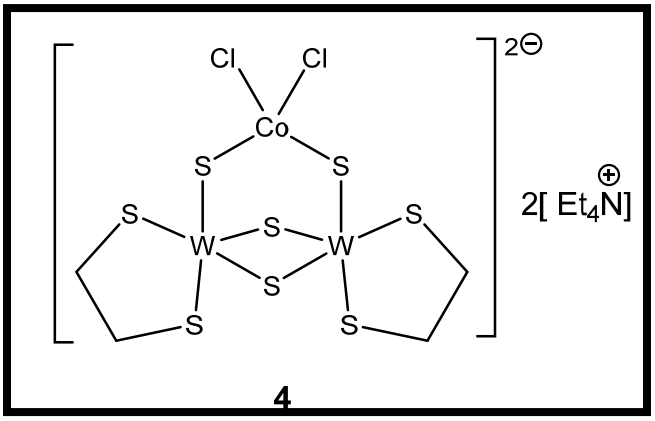

Figure 8: Structure of compound 4

2.5. Treatment of Compound 2 with $NiCl_2$

In the glovebox, to a 100-mL Schlenk tube with stir bar was added a solution of 91mg (0.1mmol) **2** in 10 mL CH_3CN. To this solution was slowly added a suspension of 18 mg (0.1 mmol) $NiCl_2$ in 5 ml CH_3CN (the $NiCl_2$ was only partially soluble). No color change was observed upon mixing. The Schlenk tube was tightly sealed, removed from the glovebox, and heated overnight (20-24 h) at about 84 ˚C in a silicone oil bath. The mixture darkened gradually upon heating. The following day, the reaction mixture was cooled to room temperature, solvent was removed on the Schlenk line without exposing the mixture to air, and the solid crude product was returned to the glovebox. In the glovebox, 10 mL CH_2Cl_2 was added to the crude product, and the mixture was filtered to give a dark red filtrate. Atop the filtrate was gently layered by 10 mL hexane, and this mixture was put in the glovebox freezer at -30 ˚C, giving crystals within 2 to 4 days. The supernatant was removed, and the crystals were then washed by hexane and dried under vacuum, yielding 0.020 g product, whose proposed structure was compound **5** below.

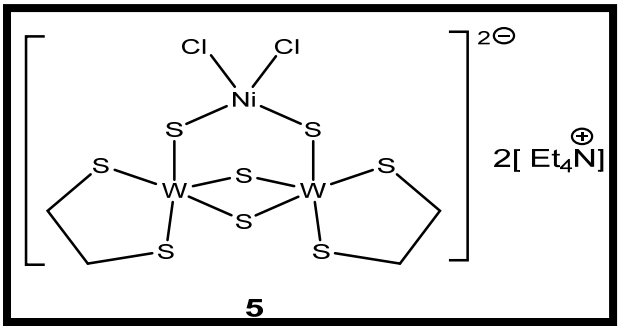

Figure 9: Structure of compound 5

2.6. Treatment of Compound 2 with $CuCl_2$

In the glovebox, to a 100-mL Schlenk tube with stir bar was added a solution of 93 mg (1mmol) **2** in 10 mL CH_3CN. To this solution was slowly added a solution of 17 mg (0.1 mmol) $CuCl_2$ in 5 mL CH_3CN. The color changed gradually upon addition from orange-red to dark orange. The Schlenk tube was tightly sealed, removed from the glovebox, and heated overnight (20-24 h) in a silicone oil bath at about 84 ˚C. The following day, the reaction mixture was cooled to room temperature, solvent was removed on the Schlenk line without exposing the mixture to air, and the solid crude product was returned to the glovebox. In the glovebox,10 mL CH_2Cl_2 was added to the crude product, which was then filtered, giving an orange-red filtrate. Atop the filtrate was gently layered 10 mL hexane, and this mixture was put in the glovebox freezer at -30 ˚C, giving crystals within 2 to 4 days. The supernatant was removed, and the crystals were washed by hexane and dried under vacuum, yielding 0.021 g product, whose proposed structure was compound **6** below.

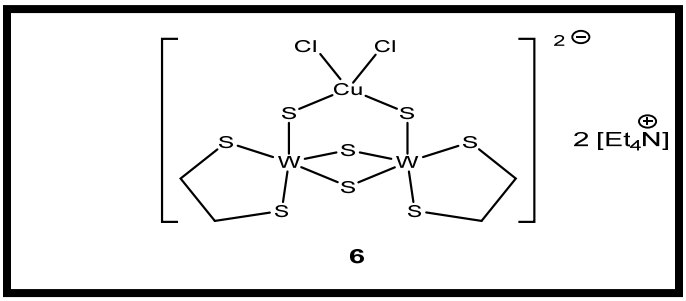

Figure 10: Structure of compound 6

CHAPTER III

RESULTS AND DISCUSSION

3.1. UV-Visible Spectra

All samples for UV-visible spectroscopy were prepared in CH_3CN solvent. The concentrations were not measured because the structures have not yet been confirmed. UV-vis spectra for the starting materials (compounds **1** and **2** and first transition-series chlorides) were obtained for comparison with resulted products.

Table 1. UV-vis spectral data

Compound	**UV-vis λ, nm**
1	453, 310, 218
2	386, 286, 215
3	355, 293, 217
4	678, 587, 375, 254
5	375
6	413, 272
$FeCl_2$	360, 311, 240
$CoCl_2$	682, 613, 589, 573, 255, 214
$NiCl_2$	301, 240
$CuCl_2$	459, 310

3.2. IR Spectra

Fourier-transform IR (FTIR) spectra were obtained using a PerkinElmer Spectrum 2 spectrometer, using attenuated total reflection (ATR) mode with neat solid samples.

Table 2: IR spectral data: w = weak, m = medium, s = strong

Compound	ν, cm^{-1}
1	2971 (m), 2892 (w), 1669 (w), 1436 (m), 1390 (m), 1170, (m), 998 (m), 397 (w), 783 (w), 522 (s), 471 (m)
2	2976 (w), 2892 (w), 1483 (m), 1446 (m), 1390 (m), 1273 (w), 1170 (m), 1002 (m), 788 (m), 503(s), 466(m)
3	2983 (w), 2948.9 (w), 1457 (s), 1405 (m), 1310.4 (w), 1184 (S), 1037 (m), 790 (s), 466 (w)
4	2983 (w), 2900 (w), 1650 (w), 1458 (s), 1397 (m), 1271 (w), 1184 (m), 944 (s), 791 (s), 500 (s), 465 (m)
5	3344 (Broad w), 2978 (w), 2891 (w), 1650 (w), 1484 (m), 1393 (m), 1271 (w), 1175 (m), 1001 (m), 944 (s), 787 (m), 726 (s), 500 (s), 465 (m)
6	2987(w), 2908 (w), 1641 (w), 1458(m) ,1384 (m),1275 (w),1175 (m), 1005 (m),944 (s), 787 (s), 630 (s), 469 (s)

This table showed the starting materials and compounds obtained. (w = weak), (m = medium), (s = strong)

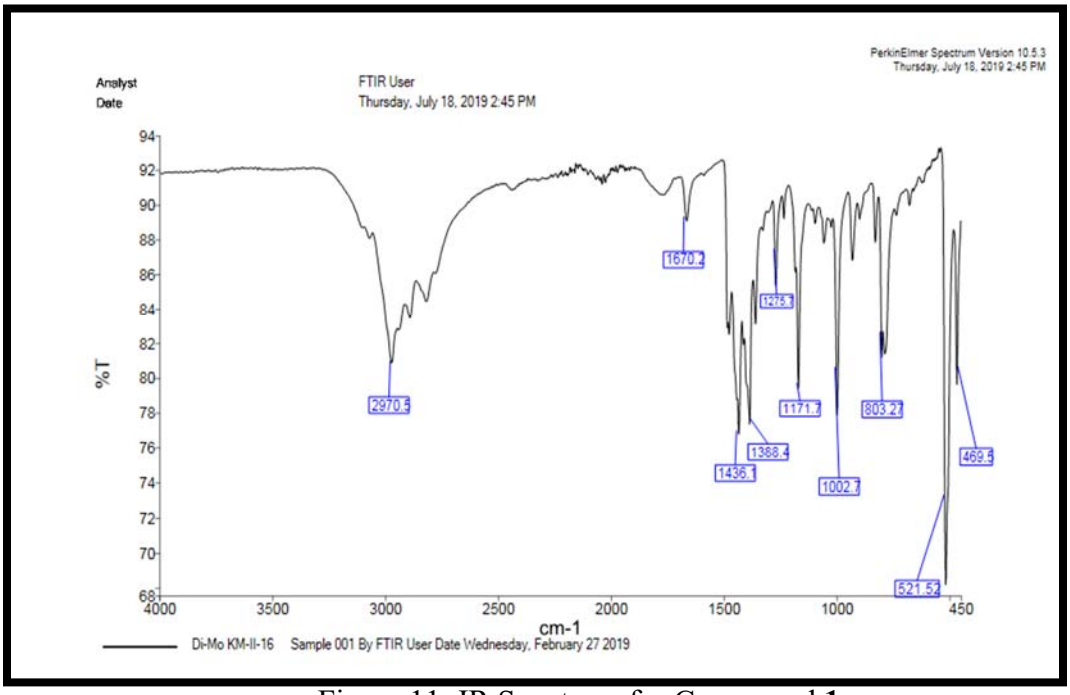

Figure 11: IR Spectrum for Compound **1**

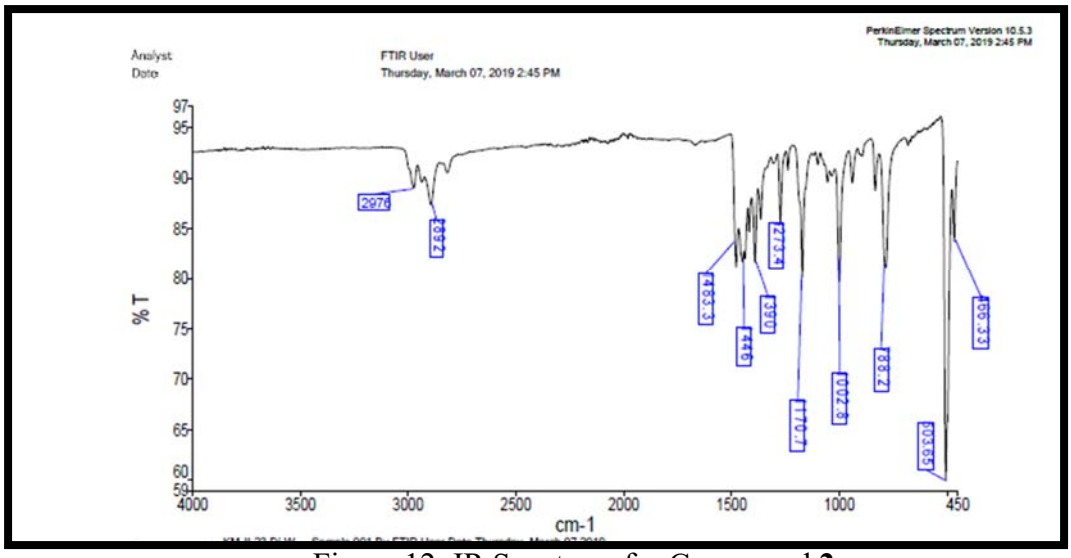

Figure 12: IR Spectrum for Compound **2**

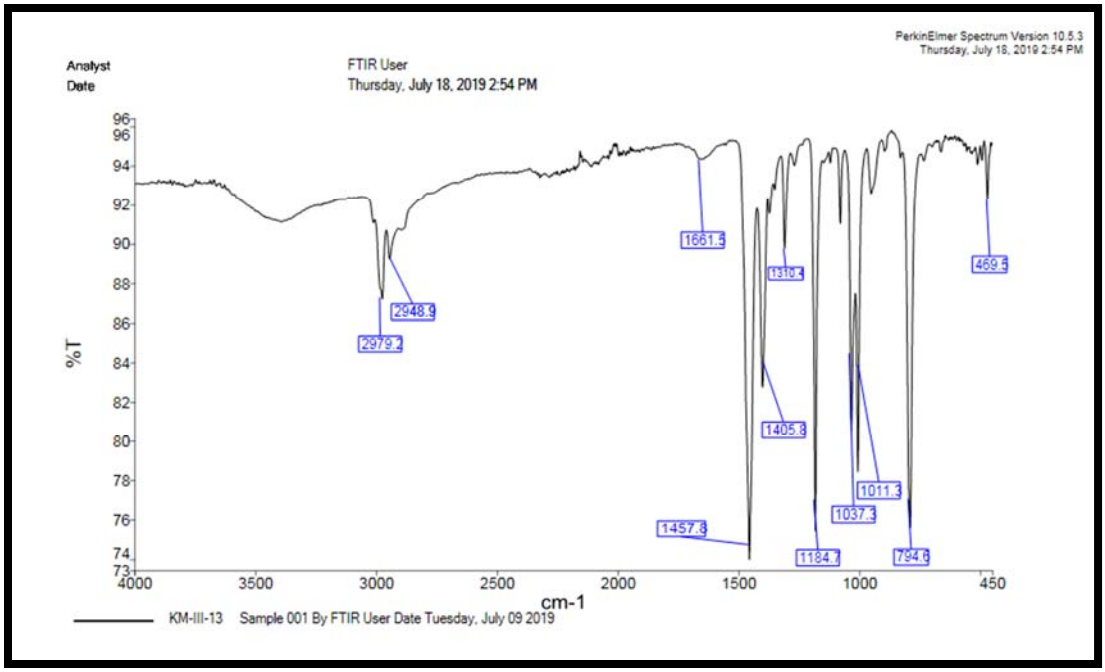

Figure 13: IR spectrum for treatment of **1** with $FeCl_2$

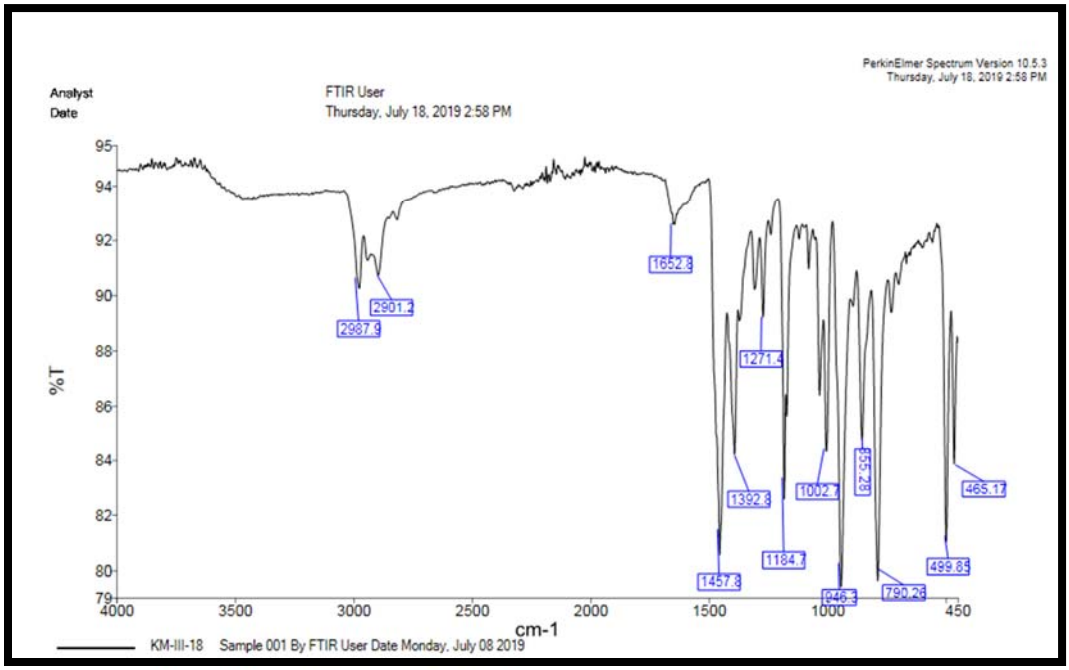

Figure 14: IR spectrum for treatment of **2** with $CoCl_2$

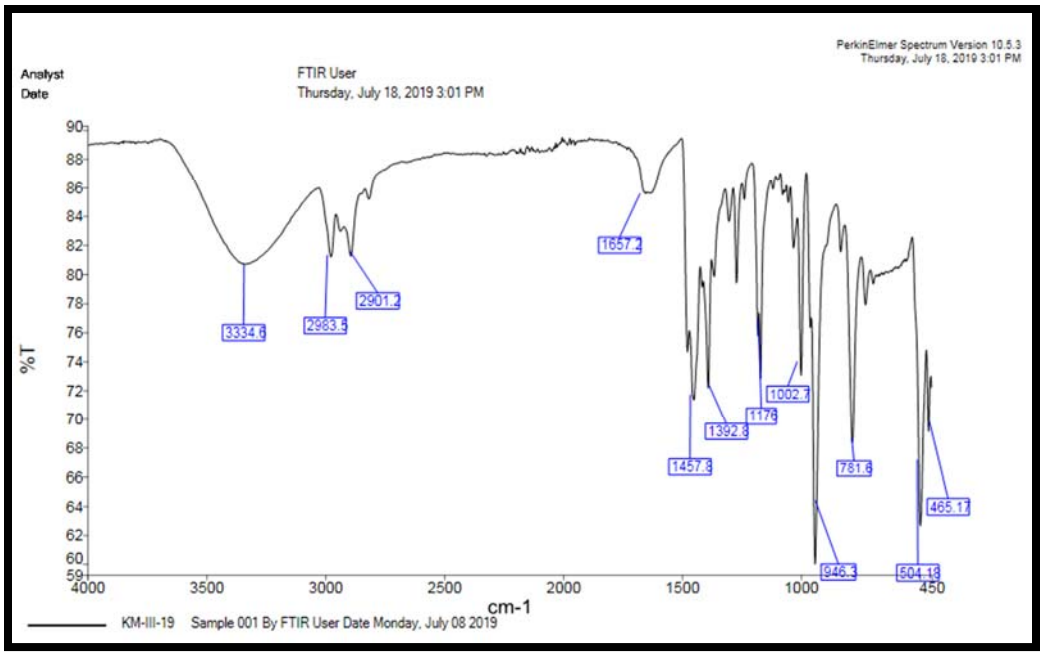

Figure 15: IR spectrum for treatment of **2** with $NiCl_2$

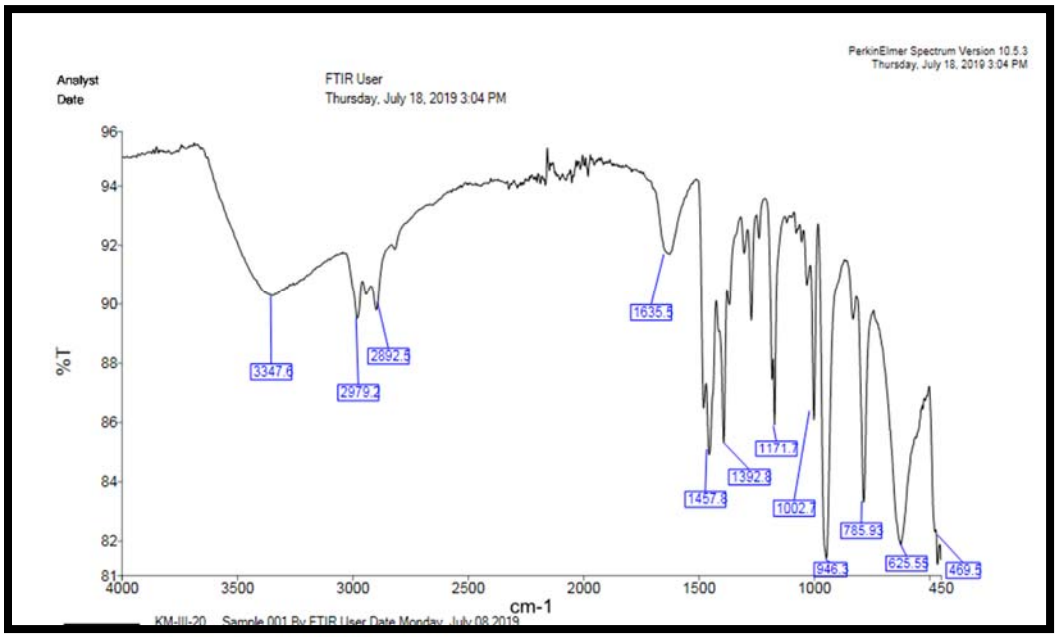

Figure 16: IR spectrum for treatment of **2** with $CuCl_2$

The bands at 471 and 522 cm^{-1} in the IR spectrum of compound **1** were assigned as Mo-S double bond stretching vibrations[21]. The bands at 466 and 503 cm^{-1} in the IR spectrum of compound **2** were assigned as W-S double bond stretching vibrations[21].

These bands would be expected to change in frequency when another metal, such as Fe, Co, Ni, or Cu, were to be bound to a sulfido ligand in one of these complexes.

3.3. Treatment of 1 with $FeCl_2$

Three peaks appeared in the UV-vis spectrum of compound **3,** formed from the reaction of compound **1** with $FeCl_2$ in acetonitrile. The peaks at 355 and 293 nm were shifted dramatically from the peaks at 453 and 310 nm seen in the UV-vis spectrum of compound 1.

There are significant differences in the IR spectra of **1** and **3**. While the spectrum of **1** shows a strong, sharp peak at 522 cm^{-1}, that of **3** instead shows a strong, sharp peak at 790 cm^{-1}. This significant shift may be due to Fe–S bonding in **3**. Also, the spectrum of **3** demonstrated another strong sharp peaks at around 1007, 1037, 1184, and 1457 cm^{-1}. On the other hand, the peaks appearing in that range, between 1000 to 1460 cm^{-1} in spectrum of **1** mentioned above were medium sharp peaks. The significant differences clearly demonstrate that we do not have unreacted **1**, that is, some reaction certainly occurred to generate a new compound or compounds. We cannot, however, confirm from the IR spectra that structure **3** is the correct one.

3.4. Treatment of 2 with $CoCl_2$

According to Table 1, the UV-vis spectrum of **4,** formed from the reaction of compound **2** with $CoCl_2$ in acetonitrile, has peaks at 678, 587, 375, and 254 nm, whose wavelengths differ significantly from those observed in the spectra of the starting materials **2** and $CoCl_2$.

Table 2 shows that the IR spectrum of **4**, displays 3 strong, sharp, peaks at 1458, 944, and 791 cm^{-1} while at 1446, 1002, 788 cm^{-1}, medium sharp peaks were appeared for

the spectrum of compound **2**. This suggests that Co(II) may be bound to the sulfido ligands on W.

3.5. Treatment of 2 with $NiCl_2$

Table 1 shows the peak in the UV-vis spectrum for compound **5**, formed from the reaction of compound **2** with $NiCl_2$ in acetonitrile. The presence of only a single peak, at 375 nm, makes this spectrum considerably different from that of either **2** or $NiCl_2$, suggesting a novel product.

Table 2 lists the frequencies in the IR spectra of compounds **5** and **2**. Comparing between IR spectra for **2** and **5**, the spectra showed the same peaks except in 3 positions. These different positions appeared, in the IR spectrum of **5**, as a weak, broad peak at 3344 cm^{-1} and weak peaks at 1650 and 1175 cm^{-1}.

3.6. Treatment of 2 with $CuCl_2$

Table 1 shows the UV-vis data for compound **6**, afforded by the reaction of compound **2** with $CuCl_2$. The spectrum of compound **6** showed two peaks at 413 and 271 nm. This variation was significantly different compared to the starting materials' peak positions, as shown in Table 1.

A comparison between the IR spectra of **2**, and **6** shows that there are three different peaks in the spectrum of **6** whose frequencies differ significantly from those of **2**, namely, a weak, broad peak at 3344 cm^{-1}, a weak, broad peak at 1641 cm^{-1}, and a weak peak at 530 cm^{-1}.

The spectra for compounds **4**, **5**, and **6**, formed by the reactions of compound **2** with MCl_2, (M = Co, Ni, Cu), showed that spectrum of compound **4** is more different

relative to compounds **6** and **5** spectra, and hence compounds **5** and **6** are similar to each other since they have almost similar peak positions.

There was also another strategy we tried for these reactions. Treatment of MCl_2, (M = Fe, Co, Ni, Cu) with $TlPF_6$, in order to precipitate the chloride as TlCl, followed by addition of either **1** or **2** yielded diffractable crystals which were suitable for X-ray experiments. X-ray data showed that the crystals were for byproducts $(Et_4N)PF_6$. Thus, we indicate that we may obtained novel products mixed with byproducts that need to be purified by another strategy.

The UV-visible spectra, whose data are presented in Table 1, demonstrate clear differences between staring materials and the products, which strongly suggest that reactions proceeded upon overnight heating. UV-vis spectra alone are not sufficient to assign the structures of compounds **3-6**. A comparison of compounds **3-6** with their starting materials highlights significant shifts in peak locations. The strong indication that reactions proceeded is valuable. X-ray structural characterization resulted by our collaborators Dr. Youngs and Dr. Stromyer showed that some crystals we brought for X-ray experiments gave a new data that was not for starting materials although they were not interesting because it is previously known compound which is Et_4NPF_6.

While it was not possible to confirm the chemical structures proposed from UV-vis and IR spectroscopy alone, it is worth considering the possible reaction products as we could not obtain diffractable crystals of novel product for X-ray structures so far. Our proposed reaction products are heterotrimetallic cluster complexes. Three neutral tetrametallic clusters derived from compound **1** were reported by Wei and coworkers[24]: when **1** was treated with two equivalents of CuBr in the presence of the ligands

bis(diphenylphosphino)methane (dppm) and pyridine (py), the results were two neutral clusters $[(edt)_2Mo_2(O)_2(\mu\text{-}S)_2Cu_2(dppm)_2]$ and $[(edt)_2Mo_2(O)_2(\mu\text{-}S_3)(\mu_3\text{-}S)Cu_2(py)_4]$, respectively. In addition, the reaction of compound **1** with 2 equivalents of CuBr, followed by the addition of a 2:1 mixture of py and dppm formed another neutral tetrametallic cluster, $[(edt)_2Mo_2(\mu\text{-}S)_2(\mu_3\text{-}S)\ Cu_2(dppm)(py)]\cdot 6py$[24].

Moreover, another neutral tetranuclear cluster was reported (figure 2). $[Ag_2Mo_2(edt)_2S_2(\mu\text{-}S)_2(dppm)_2]\cdot 3DMF$ was formed when compound **1** reacted with 2 equivalents of $Ag(CH_3CN)_4ClO_4$ in the presence of dppm[25].

An anionic tetranuclear cluster salt was prepared by You and Liu[26]. The treatment of compound **1** with two equivalents of CuCN gives rise to the anionic tetranuclear cluster salt $(Et_4N)_2[Cu_2Mo_2(edt)_2(S)_2(\mu\text{-}S)_2(CN)_2]$ (figure 3)[26].

Another cluster anion salt was prepared by Wei and coworkers, who reacted compound **1** with an equimolar amount of CuBr. The hexanuclear cluster anion salt $(Et_4N)_2[(edt)_2Mo_2(\mu\text{-}S_3)(\mu_3\text{-}S)Cu]_2\cdot 2CH_2Cl_2$ was formed by this reaction[24].

From these, we may predict that when we treated compound **1** or **2** with equimolar amounts of MCl_2, (M = Fe, Co, Ni, Cu), there is a number of possibilities for the clusters formed: they may be either trinuclear cluster anion salts, tetranuclear cluster anion salt, neutral tetranuclear cluster, or hexanuclear cluster anion salts. Structures similar to most these possibilities have been confirmed in reported compounds. However, treating compounds 1 or 2 with first-row late transition elements in their +2 oxidation states, such as Fe(II), Co(II), Ni(II), or Cu(II), is not well known. The reaction may procced to give the chemical structures proposed or the chemical structures reported when compound **1** treated by Cu(I) and Ag(I). It is difficult to predict *a priori* what the

structures are going to be, and a definitive assignment will require X-ray crystallography, in addition to spectroscopy. Below are other possible structures of the compounds prepared, in Figures17-19.

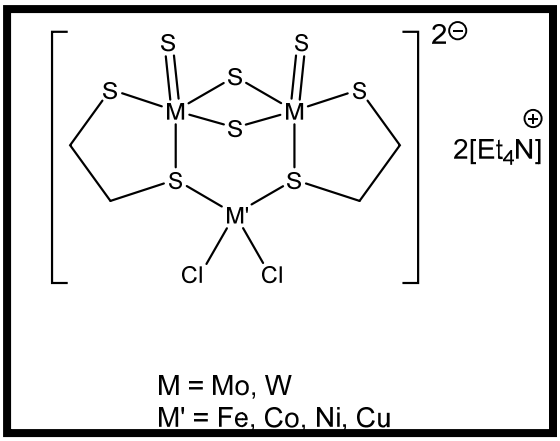

Figure 17: Structure of $(Et_4N)_2[M'Mo_2(S)_2(\mu\text{-}S)_2(edt)_2Cl_2]$

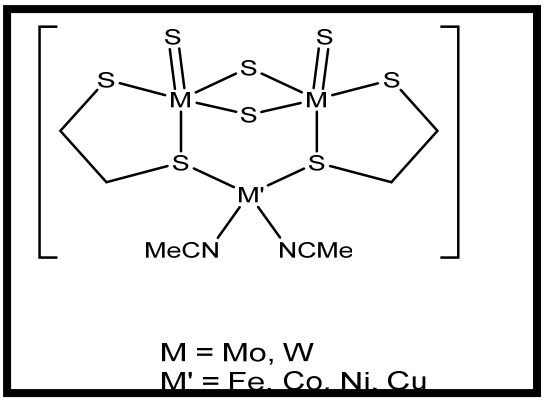

Figure 18: Structure of $[M'Mo_2(S)_2(\mu\text{-}S)_2(edt)2(CH_3CN)_2]$

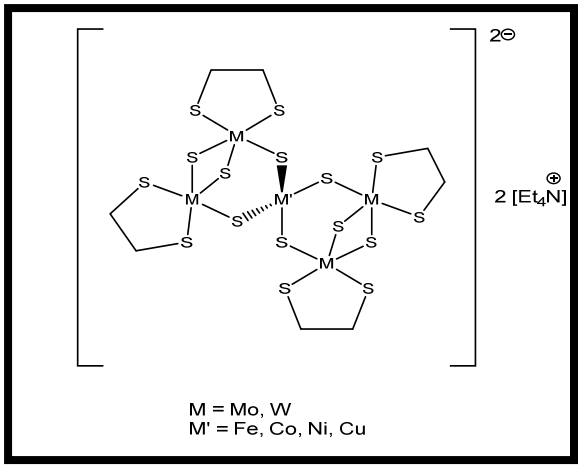

Figure 19: Structure of $(Et_4N)_2[M'(Mo_2(S)_2(\mu\text{-}S)_2(edt)_2)_2]$

CHAPTER IV

CONCLUSION

Our hypothesis of this project involved trimetallic anion cluster when compounds **1** or **2** treated by first row transition metals such as Fe(II), Co(II), Ni(II), and Cu(II). The expected results were shown in compounds **3** to **6**. Another hypothesis was that treatment of compound **1** or **2** with MCl2 (M = Fe, Co, Ni, Cu) would afford either trinuclear cluster anion salts, tetranuclear cluster anion salt, neutral tetranuclear cluster, or hexanuclear cluster anion salt, as some of them were reported in the literatures when compound 1 reacted with Cu(I), or Ag(I). UV-vis spectra were useful for comparing between the starting materials and obtained results. IR spectra showed the differences between the all compounds when compared with starting materials. However, NMR experiments were useless because the fact that the compound **1** and **2** are paramagnetic as well as all the expected results. Also, without X-ray structures, it was not possible to confirm the structures proposed by the UV-vis and IR only, and it is difficult to predict *a priori* what the structures are. Our future directions are to confirm structure of the obtained compounds and examine these complexes in medicinal chemistry because of the contribution of Mo-S and W-S complexes to fields such as bioinorganic and medicinal chemistry.

REFERENCES

(1) Cotton, F. A.; Wilkinson, G.; Murillo, C. a.; Bochmann, M. Advanced Inorganic Chemistry, 6th Edition. *Wiley-Interscience: New York*. **1999**. https://doi.org/978-0-471-19957-1.

(2) Holm, R. H.; Solomon, E. I.; Majumdar, A.; Tenderholt, A. Comparative Molecular Chemistry of Molybdenum and Tungsten and Its Relation to Hydroxylase and Oxotransferase Enzymes. *Coord. Chem. Rev.* **2011**, *255* (9–10), 993–1015. https://doi.org/10.1016/j.ccr.2010.10.017.

(3) Bigelow, S. L. Inorganic Chemistry. *J. Am. Chem. Soc.* **1908**, *30* (11), 1794–1795. https://doi.org/10.1021/ja01953a021.

(4) Mitchell, P. C. H. The Chemistry and Uses of Molybdenum: Introductory Lecture. *J. Less-Common Met.* **1974**, *36* (1–2), 3–11. https://doi.org/10.1016/0022-5088(74)90077-0.

(5) Gong, D.; Zhou, K.; Peng, C.; Li, J.; Chen, W. Sequential Extraction of Tungsten from Scheelite through Roasting and Alkaline Leaching. *Miner. Eng.* **2019**, *132* (July 2018), 238–244. https://doi.org/10.1016/j.mineng.2018.12.017.

(6) Senthilnathan, N.; Annamalai, A. R.; Venkatachalam, G. Synthesis of Tungsten through Spark Plasma and Conventional Sintering Processes. *Mater. Today Proc.* **2018**, *5* (2), 7954–7959. https://doi.org/10.1016/j.matpr.2017.11.478.

(7) Stiefel, E. Molybdenum Enzymes, Cofactors and Chemistry. *Molybdenum Enzym. cofactors Model Syst.* **1993**, No. 4. https://doi.org/10.1021/bk-1993-0535.ch001.

(8) Kisker, C.; Schindelin, H.; Rees, D. C. MOLYBDENUM-COFACTOR–CONTAINING ENZYMES: Structure and Mechanism. *Annu. Rev. Biochem* **1997**,

66, 233–267.

(9) Smedley, P. L.; Kinniburgh, D. G. Molybdenum in Natural Waters: A Review of Occurrence, Distributions and Controls. *Appl. Geochemistry* **2017**, *84*, 387–432. https://doi.org/10.1016/j.apgeochem.2017.05.008.

(10) Mcdonald, J. W.; Friesen, G. D.; Rosenhein, L. D.; Newton, W. E. <Inorganica Chimica Acta, 72 (1983) 205-210.Pdf>. **1983**, *72*, 205–210.

(11) Kawaguchi, H.; Yamada, K.; Lang, J. P.; Tatsumi, K. A New Entry into Molybdenum/Tungsten Sulfur Chemistry: Synthesis and Reactions of Mononuclear Sulfide Complexes of Pentamethylcyclopentadienyl-Molybdenum(VI) and -Tungsten(VI). *J. Am. Chem. Soc.* **1997**, *119* (43), 10346–10358. https://doi.org/10.1021/ja971725e.

(12) Ala, A.; Walker, A. P.; Ashkan, K.; Dooley, J. S.; Schilsky, M. L.; Park, F. Wilson ' s Disease. **2006**, 397–408.

(13) White, K. N.; Conesa, C.; Sánchez, L.; Amini, M.; Farnaud, S.; Lorvoralak, C.; Evans, R. W. The Transfer of Iron between Ceruloplasmin and Transferrins. *Biochim. Biophys. Acta - Gen. Subj.* **2012**, *1820* (3), 411–416. https://doi.org/10.1016/j.bbagen.2011.10.006.

(14) El-Baz, F.; Mowafy, M. E.; Lotfy, A. Study of Serum Copper and Ceruloplasmin Levels in Egyptian Autistic Children. *Egypt. J. Med. Hum. Genet.* **2018**, *19* (2), 113–116. https://doi.org/10.1016/j.ejmhg.2017.08.002.

(15) Brewer, G. J.; Askari, F.; Dick, R. B.; Sitterly, J.; Fink, J. K.; Carlson, M.; Kluin, K. J.; Lorincz, M. T. Treatment of Wilson ' s Disease with Tetrathiomolybdate : *Transl. Res.* **2009**, *154* (2), 70–77. https://doi.org/10.1016/j.trsl.2009.05.002.

(16) Brewer, G. J. Journal of Trace Elements in Medicine and Biology The Promise of Copper Lowering Therapy with Tetrathiomolybdate in the Cure of Cancer and in the Treatment of Inflammatory Disease. *J. Trace Elem. Med. Biol.* **2014**, *28* (4), 372–378. https://doi.org/10.1016/j.jtemb.2014.07.015.

(17) Lai, Y.; Sugawara, N. Outputs of Hepatic Copper and Cadmium Stimulated by Tetrathiomolybdate (TTM) Injection in Long-Evans Cinnamon (LEC) Rats Pretreated with Cadmium , and in Fischer Rats Pretreated with Copper and Cadmium. **1997**, *120*, 47–54.

(18) Hsu, P. Y.; Yen, H. H.; Yang, T. H.; Su, C. C. Tetrathiomolybdate, a Copper Chelator Inhibited Imiquimod-Induced Skin Inflammation in Mice. *J. Dermatol. Sci.* **2018**, *92* (1), 30–37. https://doi.org/10.1016/j.jdermsci.2018.08.003.

(19) Menon, S. S.; Guruvayoorappan, C.; Sakthivel, K. M.; Rasmi, R. R. Ki-67 Protein as a Tumour Proliferation Marker. *Clin. Chim. Acta* **2019**, *491* (November 2018), 39–45. https://doi.org/10.1016/j.cca.2019.01.011.

(20) STUART H., L.; DAVID E., P.; JIMMY H., Y. Preparation and Properties of the Sodium Salt of Tetrathiomolybdate(VI), $Na_2MoS_4*3.5H_20$. *Inorganica Chim. Acta* **1984**, *93*, 57–59.

(21) Cohen, S. A.; Stiefel, E. I. Dinuclear Tungsten(V) and Molybdenum(V) Compounds Containing $M_2S_2(m\text{-}S)_2^{2+}$ Cores. Synthesis and Reactivity of [N(C2H5)4]2M2Si2 (M = W or Mo) and the Crystal Structure of $[N(C_2H_5)4]_2W_2S_2(m\text{-}S)2(S4)2$. *Inorg. Chem.* **1985**, *24* (26), 4657–4662. https://doi.org/10.1021/ic00220a046.

(22) Hydrotreating. In *Applied Catalysis*; 1989. https://doi.org/10.1016/S0166-

9834(00)80813-1.

(23) Prasad, T. P.; Germany, W. THERMALDECOMPOSITION OF $(NH_4)MoO_2S_2$,$(NH4)_2MoS_4$, (NH4)2WO2S AND (NH4)WS4. *J, inorg, nucl. Chem.* **1973**, *35* (1970), 1895–1904.

(24) Kawaguchi, H.; Yamada, K.; Ohnishi, S.; Tatsumi, K. Construction of a Cyclic Tricubane Cluster $[Cp^*_2 Mo_2 Fe_2S_4]_3$ $(\mu\text{-}S_4)_3$ from the $Mo_2Fe_2S_4$ Single Cubane Component . *J. Am. Chem. Soc.* **2002**, *119* (44), 10871–10872. https://doi.org/10.1021/ja972330y.

(25) Wang, X. C.; You, X. L. Bis[M_2-Bis-(Diphenylphosphino)Methane]Bis-(M_2-Ethane-1,2-Dithiolato)-M_4-Sulfido-M_2-Sulfidodisulfidodimolybdenum(V)Disilver(I) Dimethylformamide Trisolvate. *Acta Crystallogr. Sect. E Struct. Reports Online* **2009**, *65* (12), 10461–10468. https://doi.org/10.1107/S1600536809048648.

(26) You, X. L.; Liu, Y. L. Tetra-Ethyl-Ammonium Dicyanidobis(Ethane-1,2-Dithiol-Ato)Tetra- M_3-Sulfido-Dimolybdenum(V)Dicopper(I). *Acta Crystallogr. Sect. E Struct. Reports Online* **2009**, *65* (11), 780–781. https://doi.org/10.1107/S1600536809044821.

(27) Pan, W. H.; Chandler, T.; Enemark, J. H.; Stiefel, E. I. Reactions of Tetrathiometalates, MS_4^{2-}(M = Mo, W). Syntheses and Properties of $M_2S_4^{2+}$-Containing Compounds. Structure of Bis(Tetraphenylphosphonium) Bis(μ-Sulfido)Bis(Sulfido(l, 2-Ethanedithiolato)Tungstate(V)), $[P(C_6H_5)_4]_2[W_2S_4(S_2C_2H_4)_2]$. *Inorg. Chem.* **1984**, *23* (25), 4265–4269.